J. Condensed Matter Nucl. Sci. 29 (2019) 493–502

Research Article

# Lattice Confinement of Hydrogen in FCC Metals for Fusion Reactions

Han H. Nee*, Arsen V. Subashiev and Fracsisco M. Prados-Estéves

*Target Technology Company LLC, 564 Wald, Irvine, CA 92618, USA*

**Abstract**

Clusters of H isotope atoms segregated to vacancies, divacancies and vacancy–impurity complexes in FCC metals are proposed as fuel for low energy nuclear reactions (LENR). Such clusters combine extremely high H atomic density, large values of screening potential, and as a result, a low LENR ignition energy in eV region. Besides, high average H density can be achieved due to the superabundant vacancy state (SAV) formation. These conclusions are made based on the density functional theory (DFT) modeling of these clusters, estimations of the nuclear reaction rates using experimental data for the nuclear reaction cross sections and a wide set of experimental studies of charging and recharging of various Ni samples with H and D atoms.The results were analyzed using temperature programmed desorption. The experiments confirmed extremely high loading of Ni samples with H isotopes. We discuss the problem of suitable ignition mechanisms and sustainability conditions.
 ISSN 2227-3123

*Keywords:* DFT, Divacancies, Fusion reaction rate, Ignition energy, Lattice confinement, Nickel, Screening potential

## 1. Introduction

The experimental studies of excess heat produced by thermal, electrical, laser and other types of excitation of metals charged with hydrogen isotopes revealed a high energy gain in many observations [1]. In a number of cases the released energy cannot be interpreted in terms of traditional condensed matter physics [2]. It suggests an involvement of reactions with nuclear transformations, with much higher energy release in a single reaction event. It is well understood now that the implementation of stable nuclear reactions with low excitation energy (LENR) requires: proper fuel (with high H isotope concentration), ignition (or triggering with the required energy) and achieving conditions of sustainability (which requires H isotope supply and the energy escape from the reaction zone).

The former experimental studies reached the consensus that Pd and other FCC metals can be the best candidates for the fuel. Moreover, both former and recent studies [1–3] imply an important role of structural defects for the charging of metals with hydrogen. The experimental findings were summarized in a number of reviews which stress

*Corresponding author. E-mail: hannee@targettechnology.com.

 ISSN 2227-3123

the requirement for the creation of optimal nuclear active sites (or "nuclear active environments" [4]) for the energy production.

We have explored the possibility of LENR implementation in Ni as a more practical alternative to Pd especially in the case of a large scale application. We have found that the clusters of H isotopes in Ni, as well as in Pd, segregated to vacancies and divacancies, and vacancy–impurity complexes have unique properties that can make LENR possible. First, the average concentration of H isotope ions segregated in vacancies (and divacancies) is extremely high. Second, the screening potential for H atoms in a divacancy can reach anomalously large values. Strong screening makes the required ignition energy for LENR shift down to the eV range.

The last conclusion is based on presented estimations of the reactivity and reaction rates in the H isotope clusters using experimental data for the screening potential for the nuclear fusion cross sections. At energies $\leq$10 keV a number of face-centered cubic (FCC) metals manifest huge enhancements and indicate large values of the screening potential. We suppose that these data are obtained for the samples with structural defects.

The paper is organized as follows. First, we present results of *ab-initio* modeling of hydrogen clusters bound to vacancies, divacancies and vacancy–impurity defects. Further, we discuss the screening potential for these clusters and indicate configurations for which the anomalously high values of the screening potential can be found.

We also estimate the rate of the nuclear reaction in $m$H–V clusters in Ni and Pd. The main remaining problem which was recognized long before is the possible mechanisms of ignition of the nuclear reaction. The required energy is in the eV range, far above that available from thermal excitation. Our findings are summarized in the conclusions.

## 2. Vacancies, Divacancies and Vacancy–mpurity Complexes in FCC Metals

We used Quantum Espresso Density Functional software to calculate binding energies for various structural defects, such as vacancies, interstitial H and D atoms, divacancies, vacancy–impurity complexes and clusters of H atoms segregated to vacancies and divacancies. These calculations are based on the supercell approach when a FCC lattice supercell of 32 atoms is used with periodic boundary conditions on the supercell boundaries. Technical details, such as the validation of the approach, the accuracy estimation, the choice of the pseudopotentials and so on can be found in publication [5]. To eliminate the errors due to inter-cell interactions, the results were checked for some of the structures using computations with a larger supercell of 128 atoms. Much larger computer time requirements eliminated the possibility to use a large supercell for all complexes.

The structure of the supercells with a single vacancy and a divacancy formed by two vacancies in the nearest neighbor positions are shown in Fig. 1 with an indication of the possible positions of H isotopes

segregated to the adjacent octahedral sites of the lattice. While for a vacancy all segregation sites are equivalent, for a divacancy there are four O-$c$ sites (shown in Fig. 1 by triangles) at the corner positions, two O-$s$ -sites (open squares) at "shared" sites near the divacancy center in the divacancy atomic plane (shaded by hatching) and four $t$-sites (closed squares) at the top in the upper (3-d) and lower (first) layers. Dashed lines are guides for the eyes and indicate octahedrons of O-sites). Filling of all octahedral sites suggests that the maximum occupancy is 10. Shared sites are found to have much higher segregation energy (0.4 eV) than the rest of the sites (0.3 eV). These results are in line with the previously published results for these clusters [6,7] which, however, were restricted to only a limited number of configurations for the populating of available segregation sites. The formation energy for a number of various $m$H–$V_2$ clusters for $m = 0, 1, \ldots, 10$ is shown in Fig. 2. Although the total number of clusters with different configurations is quite high ($2^{10}$) the formation energies of different clusters with the same $m$ varies within 0.2 eV, so that the slope of the dashed line in Fig. 2 is close to the average segregation energy $E_{\rm seg} = 0.3$ eV. At $m = 10$ the formation energy becomes negative, which corresponds to the state of superabundant vacancy (SAV) state formation, proposed by Fukai [8]. According to our calculations, the SAV state for Ni is different from that for Pd: the binding of two single vacancies in the divacancy (with binding energy 30 meV/vac) and the binding energy in $m$H–$V_2$ cluster are

higher than for Pd. Therefore concentration of $m$H–$V_2$ clusters in SAV phase should be comparable to that of $m$H–V clusters.

Note that the formation of SAV state in thermal equilibrium should take a long time due to the slow diffusion process of vacancies from the surface. It is accelerated at elevated temperature and pressure. However in the case

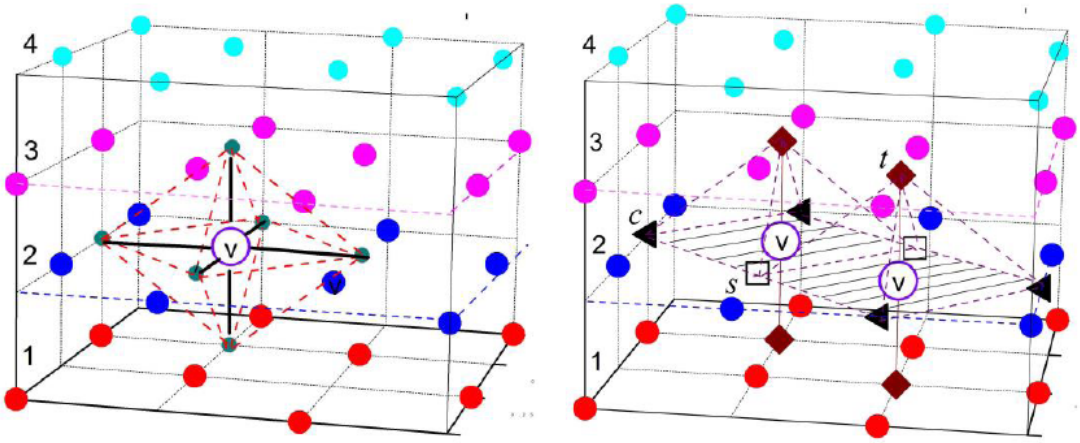


**Figure 1.** Preferred positions of H atoms at octahedral sites in a single vacancy(left panel) and a divacancy formed by emptying two nearest neighbor Ni sites (*right panel*). Shown is a 32 atom supercell with four atomic layers marked by solid dots of different colors and vacancies shown by hollow dots.

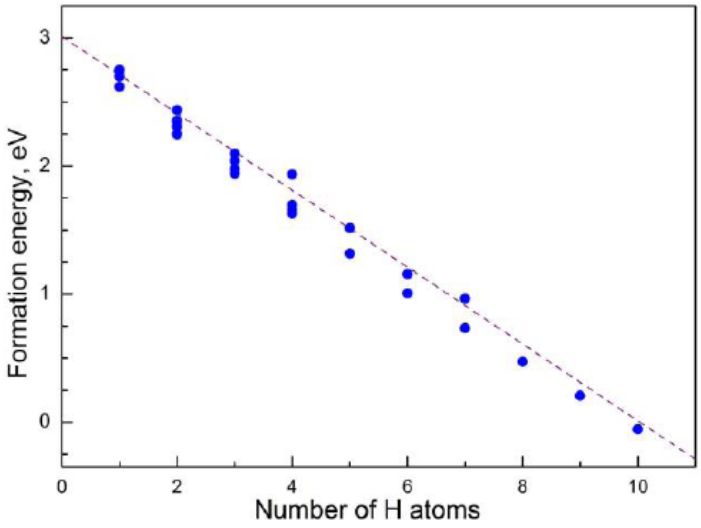


**Figure 2.** Formation energies for various $m$H–$V_2$ clusters with $m = 0, 1, 2, \ldots, 10$.

**Table 1.** Mass and particle density for different H phases as compared to that of 6H–V and 10H–$V_2$ clusters in metallic Ni and Pd.

| Phase | Mass density (g/m$^3$) | H density ($10^{22}$ at/cm$^3$) | Ref. |
|---|---|---|---|
| H (mol liquid) | 0.07 | 4.2 | [9] |
| H (mol. Solid) | 0.076 | 4.54 | [9] |
| DT ice | 0.25 | 5.6 | [10] |
| Metallic H | 0.7 | 41.9 | [11] |
| 6H–V cluster in Pd | 0.73 | 43.8 | This publ. |
| 10-$V_2$ cluster in Pd | 1.06 | 63.5 | This publ. |
| 6H-V cluster in Ni | 1.01 | 60 | [5] |
| 10-$V_2$ cluster in Ni | 1.45 | 87 | [5] |
| H in the Sun, avg. | 1.4 | 83.8 | [12] |

of an initial structure with high vacancy concentration or when the hydrogen charging process includes creation of vacancies, as shown by Staker in Appendixes A and B of his paper, in this volume [16], it can be predominant.

We have also calculated the defect formation volume, i.e. the volume into which H is segregated, and further, the average atomic density for a 6H–V and a 10H–$V_2$ clusters of segregated H atoms. The data on the hydrogen concentration in various phases and also in the hydrogen clusters are summarized in Table 1.

For a divacancy in Ni this density appears to be very high, $n = 8.7 \times 10^{23}$ at/cm$^3$, which is two times higher than that for a calculated density of metallic hydrogen and close to the average atomic density in the Sun. Somewhat smaller density, $n = 6 \times 10^{23}$ at/cm$^3$, is found for a 6H–V vacancy cluster. This fact is important for the possibility of a nuclear reaction in such clusters, since the energies of atoms in various positions inside the clusters are quite close. The density of H isotopes in similar clusters in Pd is at least 1.37 times smaller due to a larger lattice constant and its substantial increase in H charging. Calculated binding energy for the subsequent segregation in Ni varies from $\approx 0.27$ eV for $m$H–V clusters to 0.4 eV for $m$H–$V_2$ clusters and shows a sufficient stability of these clusters. For Pd these energies are $E_{\rm v} = 0.2$ eV and $E_{\rm v2} = 0.26$ eV. In both cases the SAV formation seems to be more probable in metallic Ni, than in Pd. However, in Pd it takes place in a hydride phase, rather than in the metallic phase.

Modeling of the clusters in Ni composed of a single vacancy with an impurity atom at the nearest neighbor site was also performed. We considered Al, Li and Mo impurities that can be present in catalytic Ni for technological reasons. We have found that among other impurities Li favorably increases H binding energy to a vacancy, Al does not have much effect, and Mo can have a negative effect on the SAV phase formation. Thus, the average H concentration can be further increased by doping impurities (e.g. Li) with enlarged binding energy of $m$H–V–I clusters.

We have also calculated the electronic charge distribution in $m$H–V and $m$H–$V_2$ clusters. These calculations showed that the positions of H atoms are close to the "apparent internal surface" where the drop of the metal electron density is maximal. For better understanding of the screening of the hydrogen charge it is useful to consider the redistribution of the electronic density $\delta\rho = \rho_{\rm Ni+H}\text{-}\rho_{\rm Ni}\text{-}\rho_{\rm H}$ (the change in electronic density in Ni and near H atoms due to segregation) for a cluster with segregated H atoms. It is depicted in Fig. 3 for a 10H–$V_2$ cluster and an interstitial H at the tetragonal site of Ni lattice.

Charge density contours are drawn from –0.1 to 0.1 with the interval of 0.001 electrons/Å$^3$. The redistribution results in the depletion of density of the orbitals of the nearest Ni atoms and accumulation of the excessive electronic charges on H atoms. The total accumulated charge is of about 0.1 of electron charge, and it is distributed almost spherically inside a radius of about 10 nm. This redistribution cannot be interpreted as the manifestation of anomalously high screening potential.

However, the modeling showed the possibility of hydrogen segregation into anomalous pair states with distances smaller than the 25 nm (the distance between the nearest octahedral sites). The density distribution for two of the possible configurations is presented in Fig. 4. Paired H states showed smaller distances between H atoms in divacancy

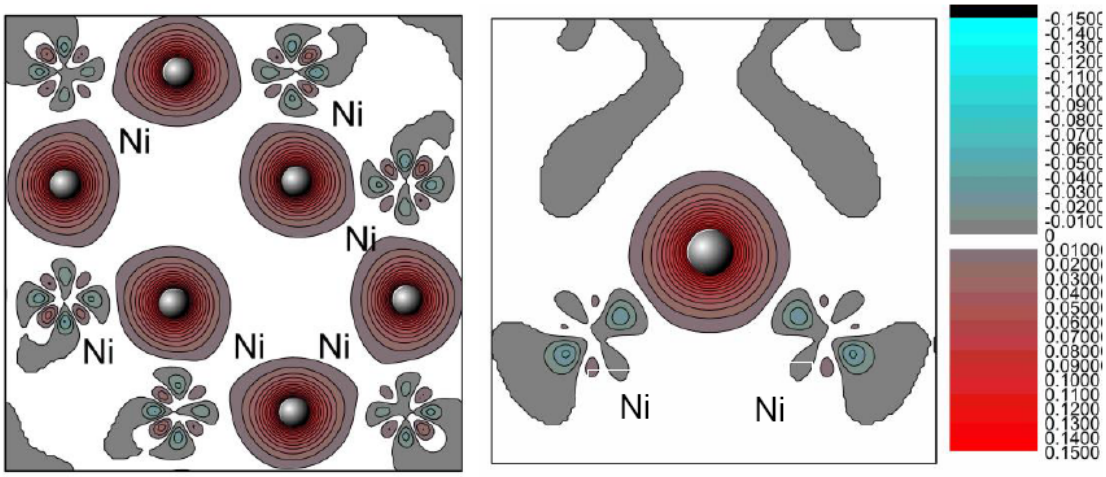


**Figure 3.** Redistribution of electron density in 10H–$V_2$ cluster in the divacancy (100) plane (*left panel*) as compared to that for a H interstitial atom at a tetragonal site (*right panel*). Blue and gray contours show depletion regions, pink and red indicate accumulation of electronic clouds around gray balls of H atoms in Ni lattice.

clusters. It can be interpreted as the reduced repulsion between the H ions at the inner surface of a divacancy. We consider it as a manifestation of a dipole–dipole, but not Coulomb, repulsion between the paired ions.

The phenomenon is known as a "supercapacitor effect", equivalent to an anomalously large screening potential experimentally found for many metallic surfaces [13]. It was found in the last decade that the capacitance of the extremely thin dielectric layers with complicated geometry is much larger than that predicted by the Helmholtz (1853) formula $C_{\mathrm{H}} = \varepsilon\varepsilon_0 S/d$, where $\varepsilon\varepsilon_0$ is the permittivity of the capacitor, $S$ is the surface area and $d$ is the distance from the charged plane to the metal surface.

The origin of the effect is the discrete nature of the charges. In deposition of a charge at the metal surface every charge initiates the charge redistribution in a metal known as an appearance of an image charge, which forms a dipole at the surface. The repulsion between the two dipoles is much weaker than the Coulomb repulsion between charges on the homogeneously charged plane. The standard estimation of the screening potential in the dense homogeneous plasma gives the value $U = Ze^2/(\varepsilon_0 a)$, where $a$ is the average distance between the charges. At the surface this distance can be several times smaller due to the dipole formation. Note that the quantitative estimation of this effect requires more detailed calculations.

To summarize, one may consider the formation of the SAV phase in FCC metals with high average H concentration and extremely large local H concentration in $m$H–V and $m$H–$V_2$ clusters as a lattice confinement.

## 3. Experimental Studies of Charging of Ni Samples with H and D Isotopes

We have studied the charging of nickel and nickel catalyst powders and also samples pressed into cylinders for further LENR experiments with Hydrogen and further recharging it with deuterium. At 83 atmospheres and 250°C the charging times were at least 24 h, but typically several days. We have studied the results with the Horiba EMGA 821 hydrogen analyzer, which enabled us to obtain the temperature programmed desorption (TPD) spectra. With the linear ramp of temperature the measured desorption rate exhibits a number of peaks which are interpreted as various bound states of hydrogen. For FCC metals the most important are three peaks associated with (i) H bound at the surface; (ii)

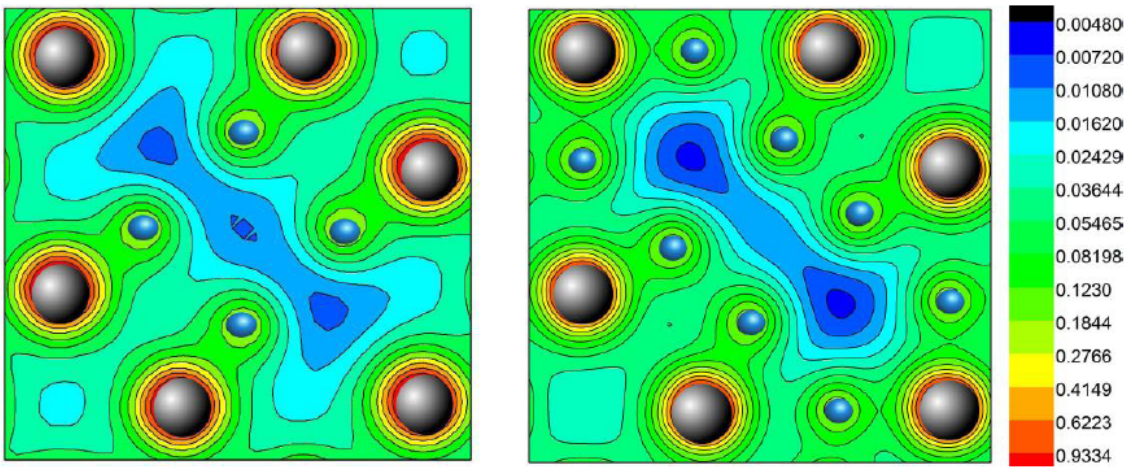


**Figure 4.** Electron charge distribution in (001) plane of $m$H-$V_2$ cluster in Ni with 4 and 8 segregated H atoms in anomalous (*pair)* positions with reduced distance between H atoms. Color panel shows density values in atomic units (1/au = 6.748 e/Å$^3$). Preferable positions are at the density ≅ 0.22 e/Å$^3$.

H segregated to single vacancies, and (iii) H segregated to divacancies. These spectra for Ni samples are presented in the Fukaibook [8] (see Fig. 5.64 in [8]). Note that the low-temperature desorption line due to surface hydrogen depends on the initial state of the surface and the heat treatment of the sample and is frequently missing if the sample is kept for some time at room temperature in Argon atmosphere.

Typical experimental desorption spectra for catalytic Ni are shown in Fig. 5 for H and D charged samples. Two characteristic peaks at 200°C and 400°C are attributed to H (D) desorption from the surface and the single vacancy clusters, correspondingly. Their position is close to that reported by Fukai [8] and others. Some shift of the peaks is attributed to a difference in the temperature ramps. The peak positions correlate with binding energies determined in *ab-initio* calculations. The intensity of the peaks in the desorption spectra can account for the concentration of the different clusters. The exact numbers vary from sample to sample. The total concentration of H(D) in the samples is very high, up to 8 at.%. If attributed to clusters with maximal occupation of octahedral sites, it corresponds to the cluster concentration of about 1 at.% (also very high).

These findings were confirmed by a large series of experiments on Ni samples and Ni samples with Li and Al impurities loaded with hydrogen with subsequent thermal desorption. Achieved average H concentration in Ni was ≈8 at.%, which corresponds to ≈1 at.% of the $m$H–V and $m$H–$V_2$ cluster concentration.

We believe that the SAV state (also known as the Fukai Phase for Pd) plays a crucial role in many excess heat experiments. In experiments with Pd electrolytic charging with D [1,3] a long charging and incubation time was found to be necessary to start excess heat production. This time was especially long at 30°C loading, but shorter at 100°C. The SAV state formation by deuterium segregated to vacancies and divacancies in the electrolytic process is a slow process of vacancy diffusion into metal from the surface and creation of divacancies. The diffusion of H isotopes goes much faster and does not add much to the incubation period.

In other cases [14,15] the initial material or the sample preparation technique includes the creation of multiple vacancies that are further stabilized into the SAV state when charged with the hydrogen isotope. For example, in the experiments of Moiser-Boss et al. [15], a Pd film was electro-deposited from PdCl solution at an extremely high electric current density. This process creates a dendritic film structure with vacancies in it. Again, D segregation is a

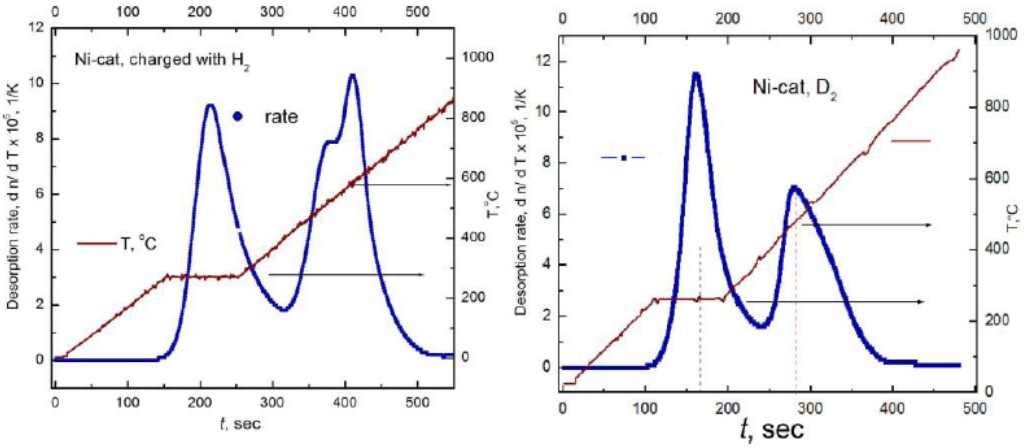


**Figure 5.** TPD spectra of Ni-catalyst charged with $H_2$ (*left panel*), to mass concentration 0.13 wt.%; right panel shows TPD spectra for Ni-catalyst sample recharged with $D_2$. Mass ratio is 0.24 wt.%.

rapid process that does not slow the SAV phase formation. So, no incubation time is required. Similar conditions are fulfilled for catalytic Ni, where due to the production process the initial concentration of vacancies is very high. The crucial role of the Fukai Phase formation for the excess heat generation in electrolytic cell experiments was recently reported by Staker [16].

The formation of the SAV is facilitated by: (i) high-current electrolysis [15], (ii) forced Kirkendall effect [17], (iii) thermal or mechanical treatments of the metal powder, e.g. quenching of metal from the molten state [18] or (iv) by low energy ion (high energy electron) beam bombardment [14] and (v) preprocessing of the metal with plastic deformation as in severe plastic deformation (SPD) or induced by loading-unloading-reloading of hydrogen isotopes with accompanying electromigration current, in addition to the electrolysis current, as detailed by Staker [16]. These techniques should be combined with fast H isotope loading to stabilize SAV phase. Importantly, the presence of SAV phase can be experimentally tested by temperature programmed desorption experiments.

## 4. Nuclear Reaction Rates

We estimated the cross sections and reactivities for the nuclear reactions between light nuclei in clusters of D segregated to vacancies or divacancies in Ni and Pd [19,20]. We assumed the thermal excitation mechanism (i.e. Maxwell energy distribution of the H isotope atoms in the cluster). The screening model based on the mean field potential of the electron cloud in the metal plasma was employed with the experimental values of the screening potential [21]. For this case the nuclear fusion reaction includes the temperature induced tunneling of ions from the high energy tail of the Maxwell distribution through the Coulomb barrier. Importantly, the effects of screening in the strongly correlated dense plasma are known to be much larger than that predicted by Debye or Thomas–Fermi models [22].

The reactivity of the reaction is defined as $\langle\sigma(v)v\rangle$ where $\sigma$ is the reaction cross section and $v$ is the relative velocity between the nuclei that will fuse in the collision. For a case of high density plasma (produced in the process of ignition) the reactivity in the cluster will be strongly enhanced due to the screening by the factor $F$ =exp($\Gamma$). The factor was scrupulously studied in a number of papers on cold fusion in astrophysical objects (see [23] for the references). At high temperatures the tunneling occurs at distances much smaller than the screening radius or average distance between the H isotope ions. For this case $\Gamma = U/(k_{\mathrm{B}}T)$. It depends only on the ratio of the value of average screening potential $U$

and the average particle energy reflected by their temperature (the local screening approximation). The enhancement factor grows exponentially at low temperatures. However, at lower temperatures and metallic densities the turning point of tunneling is shifted to larger distances between the ions, where the screening potential is reduced. Therefore the local screening approximation fails. The exponential increase is modified but still holds true until $\Gamma \leq 170$. Importantly, the corresponding maximal value of the enhancement factor can be really huge $F_{\max} = 10^{74}$. At lowered temperatures (energies) the growth of enhancement is slowed down and is given by [23]

$$F = \exp[\Gamma(1\text{–}c\Gamma^{4/3})]. \tag{1}$$

Here $c$ is a coefficient that can be estimated in a homogeneous dense Coulomb plasma model [19,23], which gave $c = 1.8 \times 10^{-4}$ for Pd and $c = 2.1 \times 10^{-4}$ for H clusters in Ni. We have calculated reactivities for D–D reactions for the deuterium clusters in Pd and Ni, using experimental values of the screening potential [22]: $U_{\mathrm{Pd}} = 800$ eV and $U_{\mathrm{Ni}} = 394$ eV. These reactivities with screening factors calculated using Eq. (1) are presented in log scale in Fig. 6 (solid lines). The reactivities in the local screening approximation, and also without screening are shown by dashed lines. Vertical dashed line indicates the applicability limit of the results. Both the screening effects and the non-local corrections result in the exponentially large variations of the reactivity values. One can further estimate the optimal excitation energy as $k_{\mathrm{B}}T_0 = U/170$, which gives the values $k_{\mathrm{B}}T_0 = 2.317$ eV for Ni, and $k_{\mathrm{B}}T_0 = 4.706$ eV for Pd. From Eq. (1) it follows that the reduced values of screening factors at the optimal energy are $F_{\mathrm{R,Pd}} = \exp(152)$, $F_{\mathrm{R,Ni}} = \exp(147)$. The corresponding reactivities are $\langle\sigma(v)v\rangle_{\mathrm{Ni}} = 1.7 \times 10^{-10}$ cm$^3$/s and $\langle\sigma(v)v\rangle_{\mathrm{Pd}} = 1.2 \times 10^{-9}$ cm$^3$/s.

We can estimate the nuclear fusion reaction rates in 6D–V and 10D–$V_2$ clusters in Pd and Ni, taking into account the density values of segregated H isotopes in monovacancies and divacancies from Table 1. Then, for a single 6D–V cluster in Ni the reaction rate is $R = 3 \times 10^{13}$1/s and $R = 4.7 \times 10^{13}$1/s for Pd. The advantage of Pd over Ni is not so large because of the higher density of segregated atoms in Ni. The high burning rate only indicates that the limiting stage of the energy production will be the H isotope diffusion and segregation to the vacancies and divacancies. These reaction rates would correspond to a very high energy production for a gram of fuel, far above any chemical sources of energy. The ignition of the nuclear reaction requires the energies in D nuclei at least several eV, which is far above what can be achieved in the thermal heating experiments. Due to the high reaction rates the vacancy clusters with segregated H are most probably the Nuclear Active Environment sites [24] for the LENR.

In the case of reaching the ignition energy, the LENR energy dissipation can be provided by the plasmon emission by the charged product particles along the escape tracks. The rate of the nuclear burning will depend on the H isotope diffusion to the vacancy cluster from the bulk and can be controlled by the ambient H pressure. Therefore, the ignited reaction could be self-sustained.

The huge remaining problem is finding a suitable ignition mechanism, since our calculation ruled out thermal excitation. In the electrolytic cell experiments, inhomogeneities of the surface structure could be a reason for the large fluctuations of local electric field. The mechanism of the energy transfer to the ions in this region remains uncertain. The other candidate is the plasmon mechanism of ignition that could provide a suitable energy range (the surface plasmon energies are $\hbar\omega_{\mathrm{p}} \cong 7$ eV). Available mechanisms of plasmon excitation are also well known (e.g. high energy electron beams [14]). However, the conversion of the plasmon energy into the energy of colliding ions remains problematic.

## 5. Conclusions

Our theoretical and experimental studies of H isotope clusters in Ni showed that $m$H–V, $m$H–$V_2$, and $m$H–V–I complexes give high H loading and an extremely high local concentration of H for the SAV metal phase. Large experimental

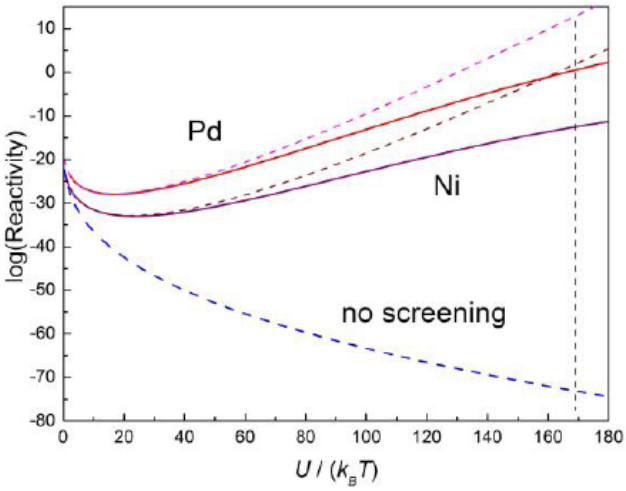


**Figure 6.** Reactivity for D–D reactions in Pd and Ni (in $cm^3/s$ units, log scale) enhanced by the screening factor $\exp(\Gamma)$, see Eq. (2), as a function of ratio $U/k_BT$; also shown is the reactivity without screening and reactivities in the local screening approximation (*dashed lines*).

values of the screening potential can be attributed to an anomalously high screening effect at the inner surface of the metal in these clusters. Our estimation of the reactivity in the conditions of optimum excitation that maximizes the screening enhancement showed that the optimal excitation energy (for the thermally enhanced tunneling through the Coulomb barrier) is in the range of 2–5 eV, making LENR ignition more plausible. Therefore, the vacancy clusters with segregated H are most probably the Nuclear Active Environment sites. The H isotope clusters can provide lattice confinement which makes these materials suitable as a LENR fuel. Finally, in our view, LENR can and should be understood and implemented within the boundaries imposed by solid state and nuclear physics.

## References

[1] M.C. H.McKubre, F.L. Tanzella, P.L. Hagelstein, K. Mullican and M. Trevithick, The need for triggering in cold fusion reactions, in *10th Int. Conf. on Cold Fusion*, P. L.Hagelstein (Ed.), Condensed Matter Nuclear Science, Word Scientific, USA, 2005. pp. 199–212.

[2] M.R. Swartz, Survey of the observed excess energy and emissions in lattice assisted nuclear reactions, *J. Scientific Exploration* **23** (4) (2009) 419–436.

[3] M.C.H. McKubre, Cold Fusion – CMNS – LENR; past, present and projected future status, *J. Condensed Matter Nucl. Sci.* **19** (2016) 183-191.

[4] E. Storms, An explanation of low-energy nuclear reactions (Cold Fusion), *J. Condensed Matter Nucl. Sci.* **9** (2012) 86–107.

[5] A. Subashiev and H. Nee, Hydrogen trapping at divacancies and impurity–vacancy complexes in nickel: first principles study, *J. Nucl. Materials* **487** (2017) 135–142.

[6] D. Tanguy, Y. Wang and D. Connetable, Stability of vacancy-hydrogen clusters in nickel from the first-principles calculations, *Acta Materialia* **78** (2014) 135–143.

[7] R. Nazarov, T. Hickel and J. Neugebauer, *Ab-initio* study of H-vacancy interactions in FCC metals: implications for the formation of superabundant vacancies, *Phys. Rev.* B **89** (2014) 144108–1–17.

[8] Y. Fukai, *The Metal-hydrogen System: Basic Bulk Properties*, 2nd edition, Springer, Berlin, 2005, pp. 147–158.

[9] J. Zhang, T.S. Fisher, P.V. Ramachandran, J.P. Gore and I. Mudawar, A review of heat transfer issues in hydrogen storage

technologies, *J. Heat Transfer* **127** (2005) 1391–1399.
[10] D.C. Wilson, P.A. Bradley, N.M. Hoffman, F.J. Swenson, D.P. Smitherman, R.E. Chrien, R.W. Margevicius, D.J. Thoma, L.R. Foreman, J.K. Hoffer, S.R. Goldman, S.E. Caldwell, T.R. Dittrich, S.W. Haan, M.M. Marinak, S.M. Pollaine and J.J. Sanchez, The development and advantages of beryllium capsules for the national ignition facility, *Phys. Plasmas* **5** (1998) 1953–1959.
[11] W.J. Nellis, Dynamic compression of materials: metallization of fluid hydrogen at high pressures, *Rep. Prog. Phys*. **69** (2006) 1479–1492.
[12] J.-L. Basdevant, J. Rich and M. Spiro, *Fundamentals of Nuclear Physics*, Springer Science and Business Media, NY, 2004, pp. 229–304.
[13] B. Skinner, M.S. Loth and B.I. Shklovskii, Capacitance of the double layer formed at the metal/ionic-conductor interface: how large can it be? *Phys. Rev. Lett.* **104** (12) (2010) 128302–128306.
[14] M. Swartz and P.L. Hagelstein, Transient vacancy phase states in palladium after high dose-rate electron beam irradiation, *J. Condensed Matter Nucl. Sci.* **14** (2014) 50–60.
[15] P.A. Moiser-Boss, S.R. Chub, M. Fleischman, M.A. Imam, M.H. Miles and S. Szpak, *Thermal and Nuclear Aspects of the Pd/$D_2O$ System*, S. Szpak and P.A. Moiser-Boss (Eds.), Vol. 1, *A decade of Research at Navy Laboratories: SPAWAR Systems Center*, San Diego, US Navy, 2002.
[16] M.R. Staker, Coupled calorimetry and resistivity measurements, in conjunction with an emended and more complete phase diagram of the palladium - isotopic hydrogen system, *J. Condensed Matter Nucl. Sci.* (2019), this volume.
[17] H.J. Fan, M. Knez, R. Sholz et al., Influence of surface diffusion on the void formation induced by the Kirkendall effect: the basic concept, *Nano Lett.* **7** (4) (2007) 993–997.
[18] W. Wycisk and M. Feller-Kniepmeier, Quenching experiments on high-purity nickel, *Phys. Stat. Sol.* (a) **37** (1) (1976) 183–191.
[19] F. Prados-Estévez, A. Subashiev and H. Nee, Nuclear fusion by lattice confinement, *J. Phys. Soc. Jpn.* **86** (7) (2017) 074201–074211.
[20] F. Prados-Estévez, A. Subashiev and H. Nee, Strong screening by lattice confinement and resultant fusion reaction rates in fcc metals, *Nucl. Instrum. Methods Phys. Res.* B **407** (2017) 67–72.
[21] F. Raiola, B. Burchard, Fülöp, Gy. Gyürky, S. Zeng, J. Cruz, A. Di Leva, B. Limata, M. Fonseca, H. Luis, M. Aliotta, H.W. Becker, C. Broggini, A. D'Onofrio, L. Gialanella, G. Imbriani, A.P. Jesus, M. Junker, J.P. Ribeiro, V. Roca, C. Rolfs, M. Romano, E. Somorjai, F. Strieder, and F. Terrasi, Enhanced electron screening in d(d,p)t for deuterated metals, *Eur. Phys. J.* A **19** (2004) 283–287, *ibid*. Enhanced d(d,p)t fusion reaction in metals, **27** (2006) 79–82.
[22] A. Huke, K. Czerski, P. Heide, G. Rupreht, N. Targosz and W. Zebrowski, Enhancement of deuteron-fusion reactions in metals and experimental implications, *Phys. Rev*. C **78** (2008) 015803–1–20.
[23] A.I. Chugunov, H.E. DeWitt and D.G. Yakovlev, Coulomb tunneling for fusion reactions in dense matter: Path integral Monte Carlo versus mean field, *Phys. Rev*. D **76** (2) (2007) 025028.
[24] E. Storms, How basic behavior of LENR can guide. a search for an explanation, *J. Condensed Matter Nucl. Sci.* **20** (2016) 100–120.